

Herding stochastic autonomous agents via local control rules and online global target selection strategies

Fabrizia Auletta¹, Davide Fiore², Michael J. Richardson³, and Mario di Bernardo⁴

Abstract—In this Letter we propose a simple yet effective set of local control rules to make a group of “herder agents” collect and contain in a desired region an ensemble of non-cooperative stochastic “target agents” in the plane. We investigate the robustness of the proposed strategies to variations of the number of target agents and the strength of the repulsive force they feel when in proximity of the herders. Extensive numerical simulations confirm the effectiveness of the approach and are complemented by a more realistic validation on commercially available robotic agents via ROS.

Keywords – Biologically-Inspired Robots, Agent-Based Systems, Autonomous Agents, Multi-Robot Systems

I. INTRODUCTION

Herding is a relevant problem in multi-robot systems, e.g. [1], [2]. In this type of problems, a set of “active” agents (the herders) need to be controlled in order to drive a set of “passive” agents (the herd) towards a desired goal region and confine them therein. Notable herding solutions are those proposed in [3]–[7]. In most cases, repulsive forces exerted by the herders on the herd are exploited to drive the behaviour of the agents that need to be corralled and, at times, cooperation among the herders (such as attractive forces between them) are used to enhance the herding process. An alternative approach, when two agents are considered, is to frame the problem as a pursuit-evasion game, as done for example in [8]–[10], where the case of one passive agent evading from one pursuer is solved by computing off-line the optimal solution of a dynamic programming problem; the case of multi-driver and multi-evader agents having been more recently analysed in [11].

In Robotics, feedback control strategies have been recently presented to solve specific herding problems and guarantee convergence of the overall system. For example, in [12] the case is considered of multiple herder agents controlling the centre of mass of a flock of passive agents by surrounding and pushing them towards a goal region. The control is

designed by modelling the aggregate dynamics of the entire flock as a unicycle. The case of a single herder agent was recently studied in [13] where by using a backstepping control strategy the herder chases a group of passive agents, switching its attention among different targets, succeeding in collecting them within a goal region of interest. This idea was further developed in [14], [15] where other control strategies and the effect of uncertainties in the herd’s dynamics were investigated.

The majority of the available herding solutions assume that target agents have a natural tendency to aggregate between themselves and flock together; an assumption we do not make in the present work. Here, we consider the case of multiple herders chasing a group of targets whose dynamics, as often happens with natural agents such as fish, birds or bacteria, is stochastic and driven by a random Brownian noise. In [16]–[19] a model for the herding agent that solves this problem is derived from experimental observations of how two human players herd a group of randomly moving agents in a virtual reality setting. As discussed in [19], the two human agents start by adopting a *search and recovery* (SR) strategy, each of them chasing the farthest agent closest to themselves and pushing it inside the desired region. Once all agents are gathered inside the goal region, most pairs of human herders were observed to switch to an entirely different containment strategy, based on exhibiting an oscillatory movement along an arc around the goal region creating effectively a “repulsive wall” for the passive agents keeping them therein [18]. To capture and reproduce this behaviour in artificial agents, a nonlinear model is proposed in [19] where the switch from SR to the oscillatory containment strategy is induced by a Hopf bifurcation triggered by a change in the distance of the herd agents from the goal region.

In this Letter, we investigate whether a simpler strategy based on local feedback control rules can drive artificial robotic agents to solve the herding problem in a similar setting to that described in [19] and address the issue of how robust this strategy is to parameter perturbations, uncertainties and unmodelled disturbances in target agent dynamics. Also, we investigate whether oscillatory containment behaviour of the herders can occur as an emerging property at the macroscopic level of the local rules we use to drive them, rather than having to be encoded in their dynamics as proposed in [19]. Moreover, we explore different herding strategies for herders to decide which target agent to chase and contain at any given time, and assess how different choices affect the overall effectiveness of the methodology we propose. Finally, we compare the proposed approach to

¹Fabrizia Auletta is with the Department of Engineering Mathematics, University of Bristol, University Walk, BS8 1TR Bristol, U.K. and also with the Department of Psychology, Faculty of Medicine, Health and Human Sciences, Macquarie University, Sydney, NSW 2109, Australia. fabrizia.auletta@bristol.ac.uk

²Davide Fiore is with the Department of Mathematics and Applications “R. Caccioppoli”, University of Naples Federico II, Via Cintia, Monte S. Angelo, 80126 Naples, Italy. davide.fiore@unina.it

³Michael J. Richardson is with the Department of Psychology, Faculty of Medicine, Health and Human Sciences, and the Center for Elite Performance, Expertise and Training, Macquarie University, Sydney, NSW 2109, Australia. michael.j.richardson@mq.edu.au

⁴Mario di Bernardo is with the Department of Electrical Engineering and Information Technology, University of Naples Federico II, Via Claudio 21, 80125 Naples, Italy. mario.dibernardo@unina.it

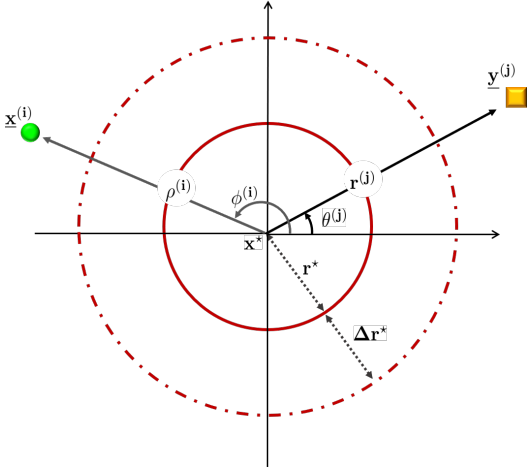


Fig. 1. Illustration of the spatial arrangement in the herding problem. The herder agent $\underline{y}^{(j)}$ (yellow square), with polar coordinates $(r^{(j)}, \theta^{(j)})$, must relocate the target agent $\underline{x}^{(i)}$ (green ball), with polar coordinates $(\rho^{(i)}, \phi^{(i)})$, in the containment region \mathcal{G} of centre \underline{x}^* and radius r^* . The buffer region \mathcal{B} , of width Δr^* , is depicted as a dashed red circle.

some others available in the literature and provide a ROS implementation of our strategy to test its ability to solve the herding problem in a more realistic robotic setting.

II. THE HERDING PROBLEM

We consider the problem of controlling N_H herder agents in order for them to drive a group of N_T target agents in the plane (\mathbb{R}^2) towards a goal region and contain them therein. We term $\underline{y}^{(j)}$ the position in Cartesian coordinates of the j -th herder in the plane and $\underline{x}^{(i)}$ that of the i -th herd (or target) agent. We denote as $(r^{(j)}, \theta^{(j)})$ and $(\rho^{(i)}, \phi^{(i)})$ their respective positions in polar coordinates as shown in Fig. 1. We assume the goal of the herders is to drive the target agents towards a circular *containment region* \mathcal{G} , of radius r^* centred at \underline{x}^* . Without loss of generality, we set \underline{x}^* to be the origin of \mathbb{R}^2 .

Assuming the herders have their own trivial dynamics in the plane, the *herding problem* can be formulated as the design of the control action u governing the dynamics of the herders given by

$$m \ddot{\underline{y}}^{(j)} = u(t, \underline{x}^{(1)}, \dots, \underline{x}^{(N_T)}, \underline{y}^{(1)}, \dots, \underline{y}^{(N_H)}), \quad (1)$$

where m denotes the mass of the herders assumed to be unitary, so that the herders can influence the dynamics of the target agents (whose dynamics will be specified in the next section) and guarantee that

$$\|\underline{x}^{(i)}(t) - \underline{x}^*\| \leq r^*, \quad \forall i, \forall t \geq \bar{t},$$

where $\|\cdot\|$ denotes the Euclidean norm; that is, all targets are contained, after some finite time \bar{t} , in the desired region \mathcal{G} .

We assume an annular *buffer region* \mathcal{B} of width Δr^* exists surrounding the goal region that the herders leave between themselves and the region where targets are contained.

In what follows we also assume that (i) herder and target agents can move freely in \mathbb{R}^2 ; (ii) herder agents have global

knowledge of the environment and of the positions of the other agents therein.

III. TARGET DYNAMICS

Taking inspiration from [17], we assume that, when interacting with the herders, targets are repelled from them and move away in the opposite direction, while in the absence of any external interaction, they randomly diffuse in the plane. Specifically, we assume targets move according to the following stochastic dynamics

$$d\underline{x}^{(i)}(t) = V_r^{(i)}(t)dt + \alpha_b dW^{(i)}(t), \quad (2)$$

where $V_r^{(i)}(t)$ describes the repulsion exerted by all the herders on the i -th target, $W^{(i)}(t) = [W_1^{(i)}(t), W_2^{(i)}(t)]^\top$ is a 2-dimensional standard Wiener process and $\alpha_b \in \mathbb{R}$ is a positive constant. We suppose the distance travelled by the targets depends on how close the herder agents are and model this effect by considering a potential field centred on the j -th herder given by $v^{(i,j)} = 1/(\|\underline{x}^{(i)} - \underline{y}^{(j)}\|)$, exerting on the targets an action proportional to its gradient [12]. Specifically, the dynamics of the i -th target agent is influenced by the reaction term

$$V_r^{(i)}(t) = \alpha_r \sum_{j=1}^{N_H} \frac{\partial v^{(i,j)}}{\partial \underline{x}^{(i)}} = \alpha_r \sum_{j=1}^{N_H} \frac{\underline{x}^{(i)}(t) - \underline{y}^{(j)}(t)}{\|\underline{x}^{(i)}(t) - \underline{y}^{(j)}(t)\|^3}, \quad (3)$$

where $\alpha_r \in \mathbb{R}$ is a positive constant. Possible modelling uncertainties in the repulsive reaction term (3) can be seen as being captured by the additional noisy term in (2).

Notice that according to (3) every target feels the influence of all the herders. Nevertheless, we assume that each herder only chases one target at a time as explained below. The position of the i -th target when it is chased by the j -th herder will be denoted as $\tilde{\underline{x}}^{(i,j)}$ or in polar coordinates as $(\tilde{\rho}^{(i,j)}, \tilde{\phi}^{(i,j)})$.

IV. HERDER DYNAMICS AND CONTROL RULES

Our solution to the herding problem consists of two layered strategies; (i) a target selection strategy through which herders decide what target to chase and (ii) a local control law driving the motion of the herder towards the target it selected, and pushing it inside the goal region.

A. Local control strategy

For the sake of comparison with the strategy presented in [17], [19], we express the control law we propose to drive each herder in polar coordinates. Albeit not resulting in the shortest possible path travelled by the herders, this controller in polar coordinates ensures circumnavigation of the goal region, avoiding targets already contained therein from being scattered around. Specifically, the control input to the j -th herder dynamics (1) is defined as $u^{(j)}(t) = u_r^{(j)}(t) \hat{r}_j + u_\theta^{(j)}(t) \hat{\theta}_j$, where $\hat{r}_j = [\cos \theta^{(j)}, \sin \theta^{(j)}]^\top$ and $\hat{\theta}_j = \hat{r}_j^\perp$ are unit vectors, and its components are chosen as

$$u_r^{(j)}(t) = -b_r \dot{r}^{(j)}(t) - \mathcal{R}(\tilde{\underline{x}}^{(i,j)}, t), \quad (4)$$

$$u_\theta^{(j)}(t) = -b_\theta \dot{\theta}^{(j)}(t) - \mathcal{T}(\tilde{\underline{x}}^{(i,j)}, t), \quad (5)$$

where the feedback terms $\mathcal{R}(\tilde{x}^{(i,j)}, t)$ and $\mathcal{T}(\tilde{x}^{(i,j)}, t)$ are elastic forces that drive the herder towards the chased target i and push it towards the containment region \mathcal{G} . Such forces are chosen as

$$\mathcal{R}(\tilde{x}^{(i,j)}, t) = \epsilon_r \left[r^{(j)}(t) - \xi^{(j)}(t) (\tilde{\rho}^{(i,j)}(t) + \Delta r^*) - (1 - \xi^{(j)}(t)) (r^* + \Delta r^*) \right], \quad (6)$$

$$\mathcal{T}(\tilde{x}^{(i,j)}, t) = \epsilon_\theta \left[\theta^{(j)}(t) - \xi^{(j)}(t) \tilde{\phi}^{(i,j)}(t) \right], \quad (7)$$

with $\xi^{(j)}(t) = 1$, if $\tilde{\rho}^{(i,j)}(t) \geq r^*$, and $\xi^{(j)}(t) = 0$, if $\tilde{\rho}^{(i,j)}(t) < r^*$, so that the herder is attracted to the position of the i -th chased target $\tilde{x}^{(i,j)}$ (plus a radial offset Δr^*) when the current target is outside the containment region ($\xi^{(j)} = 1$) or to the boundary of the buffer region otherwise ($\xi^{(j)} = 0$). Note that the control laws (4)-(5) are much simpler than those presented in [17] as they do not contain any higher order nonlinear term nor are complemented by parameter adaptation rules (see [17] for further details).

B. Target selection strategies

The local control rules for the j -th herder depend on the target being chased. It is therefore essential to design and compare different target selection strategies that multiple herders can adopt when solving collectively the same herding problem, i.e., when $N_H \geq 2$. Rather than solving an off-line or on-line optimisation problem as in [20], here we focus on deriving a set of strategies that exploit the spatial distribution of the herders allowing them to cooperatively select their target agents without requiring any computationally expensive optimisation problem to be solved on-line. We consider four different target selection strategies (or herding strategies) as described below, starting from the simplest case where herders globally look for the target farthest from the goal region. A graphical illustration of the four strategies is reported in Fig. 2 for $N_H = 3$ herders.

a) *Global search strategy (no plane partitioning)*: Each herder selects the farthest target agent from the containment region which is not currently selected by any other herder (Fig. 2(a)).

b) *Static arena partitioning*: At the beginning of the trial and for all of its duration, the plane is partitioned in N_H circular sectors of width equal to $2\pi/N_H$ rad centred at x^* . Each herder is then assigned one sector to patrol and selects the target therein that is farthest from \mathcal{G} (Fig. 2(b)). Note that this is the same herding strategy used in [17].

c) *Dynamic leader-follower target selection strategy*: At the beginning of the trial, herders are labelled from 1 to N_H in anticlockwise order starting from a randomly selected herder which is assigned the *leader* role. The leader starts by selecting the farthest target from \mathcal{G} whose angular position $\tilde{\phi}^{(i,1)}$ is such that

$$\tilde{\phi}^{(i,1)} \in \left(\theta^{(1)}(t) - \frac{1}{2} \frac{2\pi}{N_H}, \theta^{(1)}(t) + \frac{1}{2} \frac{2\pi}{N_H} \right],$$

where $\theta^{(1)}(t)$ is the angular position of the leader at time t . Then, all the other *follower* herders ($j = 2, \dots, N_H$), in

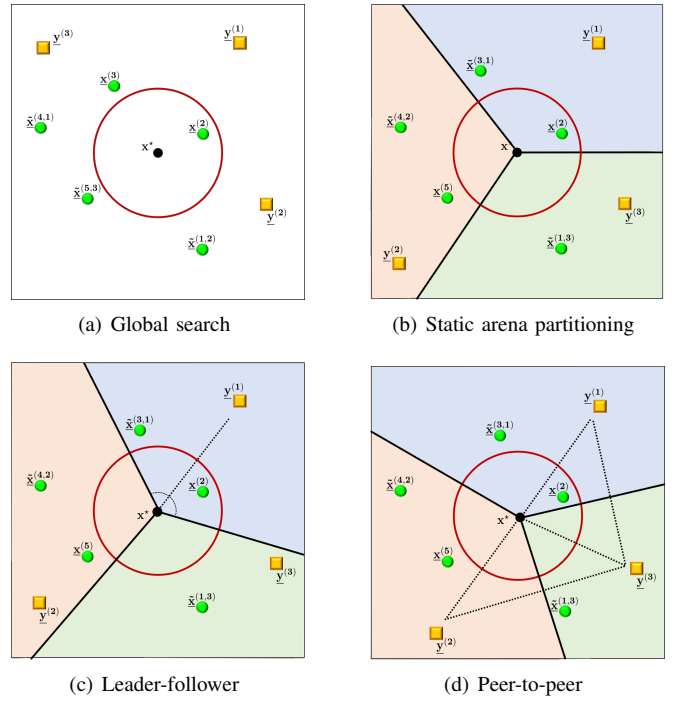


Fig. 2. Graphical representation of the target selection strategies. Herders are depicted as yellow squares, targets as green balls. The colours in which the game field is divided correspond to regions assigned to different herders. Herder $y^{(j)}$ is currently chasing target agent $\tilde{x}^{(i,j)}$, while target $\tilde{x}^{(i)}$ is not chased by any herder.

ascending order, select their targets as the agents farthest from \mathcal{G} such that

$$\tilde{\phi}^{(i,j)} \in \left(\theta^{(1)}(t) - \frac{1}{2} \frac{2\pi}{N_H} + \zeta^{(j)}, \theta^{(1)}(t) + \frac{1}{2} \frac{2\pi}{N_H} + \zeta^{(j)} \right],$$

with $\zeta^{(j)} = 2\pi(j-1)/N_H$. As the leader chases the selected target and moves in the plane, the partition described above changes dynamically so that a different circular sector with *constant* angular width $2\pi/N_H$ rad is assigned to each follower at each time instant. In Fig. 2(c) the case is depicted for $N_H = 3$ in which the sector $(\theta^{(1)} - \frac{\pi}{3}, \theta^{(1)} + \frac{\pi}{3}]$ is assigned to the leader herder while the rest of the plane is assigned equally to the other two herders.

d) *Dynamic peer-to-peer target selection strategy*: At the beginning of the trial herders are labelled from 1 to N_H as in the previous strategy. Denoting as $\zeta_j^+(t)$ the angular difference between the positions of herder j and herder $(j+1) \bmod N_H$ at time t , and as $\zeta_j^-(t)$ that between herder j and herder $(j+N_H-1) \bmod N_H$ at time t , then herder j selects the farthest target from \mathcal{G} whose angular position is such that

$$\tilde{\phi}^{(i,j)} \in \left(\theta^{(j)}(t) - \frac{\zeta_j^-(t)}{2}, \theta^{(j)}(t) + \frac{\zeta_j^+(t)}{2} \right].$$

Unlike the previous case, now the width of the circular sector assigned to each herder is also dynamically changing as it depends on the relative angular positions of the herders in the plane.

A crucial difference between the herding strategies presented above is the nature (local vs global) and amount of information that herders must possess to select their next target. Specifically, when the *global search strategy* is used, every herder needs to know the position $\underline{x}^{(i)}$ of every target agent in the plane, not currently selected by other herders. In the case of the *static arena partitioning* instead a herder needs to know its assigned (constant) circular sector together with the position $\underline{x}^{(i)}$ of every target agent in the sector.

For the dynamic target selection strategies, less information is generally required. Indeed, in the *dynamic leader-follower strategy* the herders, knowing N_H , can either self-select the sector assigned to themselves (if they act as leader) or self-determine their respective sector by knowing the position of the leader $\underline{y}^{(1)}(t)$. Similarly in the *dynamic peer-to-peer strategy* herders can self-select their sectors by using the angles $\zeta_j^+(t)$ and $\zeta_j^-(t)$.

Therefore, static strategies are less information efficient than dynamic target selection algorithms which in general mostly require local rather than global information, as for example only positions of the target agents located inside the sector assigned to each herder.

Remark. *Note that in the unlikely event of perfect radial alignment of the herder and the target it is chasing, the herder might push the target away, rather than towards the goal region. Despite its rare occurrence, such an event can be avoided by extending the herder dynamics by an extra term as shown in the Appendix II.*

V. NUMERICAL VALIDATION

The herding performance of the proposed control strategy has been evaluated through a set of numerical experiments aimed at (i) assessing its effectiveness in achieving the herding goal; (ii) comparing the use of different target selection strategies; (iii) studying the robustness of each strategy to parameter variations. The implementation and validation of the strategy in a more realistic robotic environment is reported in the next section where ROS simulations are included.

A. Performance Metrics

We defined the following metrics (see Appendix I for their definitions) to evaluate the performance of different strategies. Specifically, for each of the proposed strategies we computed the (i) gathering time t_g , (ii) the average length d_g of the path travelled by the herders until all targets are contained, (iii) the average total length d_{tot} of the path travelled by herders during all the herding trial, (iv) the mean distance D_T between the herd's centre of mass and the centre of the containment region, and (v) the herd agents' spread $S\%$.

Note that *lower* values of t_g correspond to *better* herding performance; herders taking a shorter time to gather all the target in the goal region. Also, *lower* values of D_T and $S\%$ correspond to a *tighter* containment of the target agents in the goal region while *lower* values of d_g and d_{tot} correspond

TABLE I
AVERAGE PERFORMANCE AND EMERGING BEHAVIOURS OF HERDERS FOR DIFFERENT TARGET SELECTION STRATEGIES OVER 50 TRIALS.

	Global	Static	Leader-follower	Peer-to-peer
$N_H = 2$				
t_g [a.u.]	8.52	15.19	15.31	13.34
d_g [a.u.]	139	102	92	143
d_{tot} [a.u.]	841	493	423	418
D_T [a.u.]	1.26	1.44	1.46	1.29
$S\%$ [%]	0.15	0.18	0.21	0.21
COC pairs [%]	100	100	2	78
$N_H = 3$				
t_g [a.u.]	5.88	19.60	11.23	10.11
d_g [a.u.]	88	227	84	59
d_{tot} [a.u.]	1242	814	885	932
D_T [a.u.]	0.61	1.29	0.78	0.78
$S\%$ [%]	0.13	0.39	0.24	0.91

to a *more efficient* herding capability of the herders during the gathering and containment of the agents.

When a pair of herders are considered, we also assessed, following [18], whether coordinated oscillatory motion of the herders emerged as a result of the control strategies we adopt in this Letter. Specifically, we analysed the power spectra of the herders' motion and identified it as oscillatory if the dominant frequency of the spectrum was higher than a certain threshold (see Appendix I for more details).

B. Performance analysis

We carried out 50 simulation trials with $N_T = 7$ target agents and either $N_H = 2$ or $N_H = 3$ herders, starting from random initial conditions. (All simulation parameters and a description of simulation setup adopted here are reported in Appendix II.)

The results of our numerical investigation are reported in Tab. I. As expected, when herders search globally for agents to chase, their average gathering and total paths, d_g and d_{tot} , are notably longer than when dynamic target selection strategies are used, pointing out that this strategy is going to be the least efficient when implemented.

As regards the aggregation of the herd agents in terms of D_T and $S\%$, all strategies presented comparable results. On the other hand, dynamic strategies showed consistently shorter gathering times t_g and travelled distances d_g than the static target selection strategies. In particular, in the case of three herders ($N_H = 3$), the peer-to-peer strategy exhibited values of t_g and d_g which are 50% and 74% smaller, respectively, than the static partitioning one. Therefore, we find that in general higher level of cooperation between herders and a more efficient coverage of the herding area, as those guaranteed by dynamic strategies, yield an overall better herding performance which is more suitable for realistic implementations in robots or virtual agents which are bound to move at limited speed. In most scenarios with two herders ($N_H = 2$) we tested, oscillatory motion of the herders emerges spontaneously without the need of including extra nonlinear terms in the model as done in [19] (see Fig. 3 for an example of spectral classification). Specifically, we find

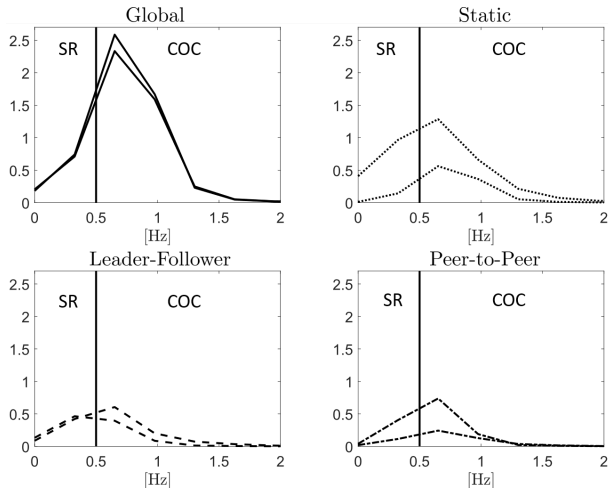


Fig. 3. Comparison of power spectra exhibited by $N_H = 2$ herders adopting different target selection strategies in a successful trial. Peak values of power spectrum are used to classify the behaviour in search and recovery (SR) or coupled oscillatory containment (COC) (see Appendix I). Herders not dividing (panel a), statically dividing (panel b) and cooperatively dividing (panel d) the game field have a peak frequency on the right side of the threshold $\omega_c = 0.5$ Hz and their coupled behaviours are classified as COC. On the other hand, herders adopting the leader-follower strategy (panel c) have peak frequencies on both sides as the leader herder mostly engage in a non-oscillatory behaviour and the follower herder in a oscillatory one (see Tab. I).

periodic motion to emerge in all the trials with both herders moving around the containment region as also observed when pairs of humans are asked to herd agents in a virtual reality setting, see [19] for further details.

C. Robustness analysis

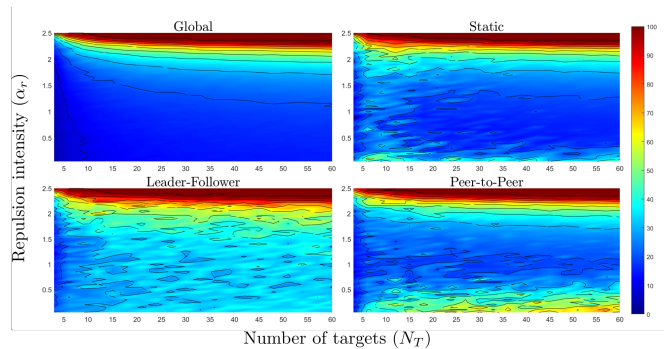
Next, we analysed the robustness of the proposed herding strategies to variations of the herd size and of the magnitude of the repulsive reaction to the herders exhibited by the target agents (Fig. 4). Specifically, we vary N_T between 3 and 60 and the repulsion parameter α_r in (3) between 0.05 and 2.5, while keeping $N_H = 2$. Strikingly, we find that all strategies succeed in herding up to 60 agents in a large region of parameter values [see the blue areas in Fig. 4(a)].

The global strategy where herders patrol the entire plane is found as expected to be the least efficient in terms of total distance travelled by the herders (Fig. 4(b)); the dynamic peer-to-peer strategy offering the best compromise and robustness property in terms of containment performance (see Fig. 4(a)) and efficiency (see Fig. 4(b)).

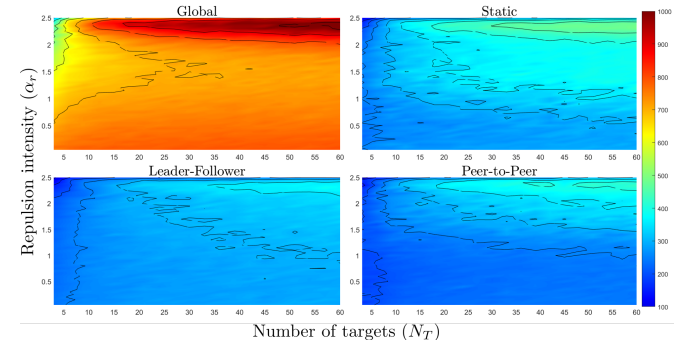
D. Comparison with other approaches

We compare our proposed herding strategy with other two solutions presented in the literature, by considering as a benchmark scenario the case of $N_H = 3$ herders chasing $N_T = 7$ targets.

The herder model in [13] was adapted to this scenario, while the model in [12] was applied as is. Specifically, the model in [13] was originally designed to drive a *single* herder to chase multiple targets by switching between one and another according to some dwell-time condition. To apply



(a) Gathering time t_g . Lower values correspond to faster herding.



(b) Total distance travelled d_{tot} . Lower values correspond to more efficient herding.

Fig. 4. Robustness analysis of the proposed herding strategies for two herders ($N_H = 2$) to variation of herd size N_T and repulsive reaction coefficient α_r . N_T was varied between 3 and 60 agents, with increments equal to 3, while α_r between 0.05 and 2.5, with increments equal to 0.05. For each pair (N_T, α_r) the corresponding metric was averaged over 15 simulation trials starting with random initial positions. The coloured plots were obtained by interpolation of the computed values.

this model to our benchmark scenario, we assume that each of the herders chases only one target at the time without coordinating with the other herders.

In all simulations the dynamics of the targets has been set as in (2). Notice that in [13] targets' dynamics is assumed to be deterministic but uncertain, while in [12] targets have noisy dynamics but they exhibit an aggregating behaviour, or flocking, that is not considered here. Performance averaged over 25 trials are shown in Tab. II. The relative poorer performance of these strategies when compared to ours can be explained by noticing that the model in [13] lacks coordination among multiple herders, while in the control solution in [12] heavily relies on flocking among target agents which is not required in our case of interest.

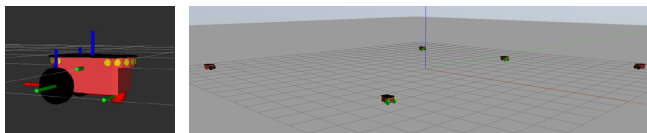
Furthermore, both models' performance is affected by the stochastic, rather than deterministic, scattering dynamics of the target agents we consider here, further confirming the effectiveness of our approach when deployed in this type of scenarios.

VI. VALIDATION IN ROS ENVIRONMENT

To validate the strategies we propose in a more realistic robotic setting, we complemented the numerical simulation

TABLE II
AVERAGE PERFORMANCE OF HERDERS FOR DIFFERENT HERDING
MODELS OVER 25 TRIALS.

	Model [13]	Model [12]	Leader-follower	Peer-to-peer
$N_H = 3$				
t_g [a.u.]	100	100	8.75	8.77
d_g [a.u.]	297.66	7.95	65.97	68.04
d_{tot} [a.u.]	297.66	7.95	813.24	908.53
D_T [a.u.]	2.94	8.17	0.68	0.7
$S_{\%}$ [%]	3.79	35.71	0.18	0.26



(a) Robot agent (b) Simulated environment

Fig. 5. Overview of Gazebo-ROS application, with 3D model of the Pioneer 3-DX robot (a) and a landscape view of the simulated environment (b).

presented in Sec. V with their ROS [21] implementation¹ as described below. We used the Gazebo software package² to test the designed control architecture on accurate 3D models of commercial robots to simulate their dynamics and physical interaction with the virtual environment.

We considered a scenario where $N_T = 3$ targets need to be herd by $N_H = 2$ robotic herders. All agents were chosen to be implemented as Pioneer 3-DX [22], a commercially available two-wheel two-motor differential drive robot whose detailed model is available in Gazebo (see Fig. 5). The desired trajectories for the robots are generated by using equations (2) and (4)-(7) for the target and herder robots, respectively, which are used as reference signals for the on-board inner control loop to generate the required tangential and angular velocities (see Appendix III for further details).

Examples of ROS simulations are reported in Fig. 6 where all the target selection strategies that were tested (static arena partitioning, leader-follower, peer-to-peer) were found to be successful with herder robots being able to gather all the target robots in the containment region. Fig. 6 also shows that the angular position of the herders remain within the bounds defining the sector of the plane assigned to them for patrolling. The only exception is found in panel Fig. 6(e) where the follower herder temporarily exceeds its bounds.

VII. CONCLUSIONS

We presented a control strategy to solve the herding problem in the scenario where a group of multiple herders is chasing a group of stochastic target agents. Our approach is based on the combination of a set of local rules driving the herders according to the targets' positions and a global herding strategy through which the plane is partitioned among the herders, who then select the target to chase in the sector assigned to them either statically or dynamically. Our

¹Code available on <https://github.com/diBernardoGroup/HerdingProblem>

²http://wiki.ros.org/gazebo_ros_pkgs

results show the effectiveness of the proposed strategy both via numerical simulations and by means of a more realistic implementation in ROS on commercially available robotic agents. Interestingly, our numerical evidence suggests that the oscillatory motions of herders observed in experiments with human players [19] may emerge from the local rules of interaction between herders and target agents and do not need to be explicitly encoded in the mathematical model describing their dynamics.

APPENDIX I PERFORMANCE METRICS

Denote with $\mathcal{X}(t) := \{i : \|\underline{x}^{(i)}(t) - \underline{x}^*\| \leq r^*\}$ the set of targets which are contained within the goal region \mathcal{G} at time t . Moreover, denote with $[0, T]$ the time interval over which the performance metrics are evaluated. The following metrics are used in the Letter to evaluate the proposed herding strategies.

a) **Gathering time:** defined as the time instant $t_g \in [0, T]$ such that all the target agents are in the containment region for the first time.

b) **Distance travelled by the herders:** which measures the mean in time and among herders of the distance travelled by the herders during the time interval $[0, t]$. It is defined as

$$d(t) := \frac{1}{N_H} \sum_{j=1}^{N_H} \frac{1}{t} \left(\int_0^t \|\dot{\underline{x}}^{(j)}(\tau)\| d\tau \right).$$

Therefore, $d_g := d(t_g)$, and $d_{tot} := d(T)$. A smaller average distance travelled indicates better efficiency of the herders in solving the task.

c) **Herd distance from containment region:** which measures the herders ability to keep the herd close to the containment region, with centre \underline{x}^* . It is defined as the mean in time of the Euclidean distance between the centre of mass of the herd and the centre of the containment region, that is

$$D_T := \frac{1}{T} \int_0^T \left\| \left(\frac{1}{N_T} \sum_{i=1}^{N_T} \underline{x}^{(i)}(\tau) \right) - \underline{x}^*(\tau) \right\| d\tau.$$

A smaller average distance indicates better ability of the herders to keep the herd close to the containment region.

d) **Herd spread:** measuring how much scattered the herd is in the game field. Denote as $\text{Pol}(t)$ the convex polygon defined by the convex hull of the points $\underline{x}^{(i)}$ at time t , that is, $\text{Pol}(t) := \text{Conv}(\{\underline{x}^{(i)}(t), i = 1, \dots, N_T\})$. Then, the herd spread S is defined as the mean in time of the area of this polygon, that is

$$S := \frac{1}{T} \int_0^T \left(\int_{\text{Pol}(\tau)} d\underline{x} \right) d\tau.$$

Lower values corresponds to a more cohesive herd and consequently better herding performance. The herd spread can also be evaluated with respect to the area of the containment region, $A_{cr} = \pi(r^*)^2$, as $S_{\%} = S/A_{cr} \cdot 100$.

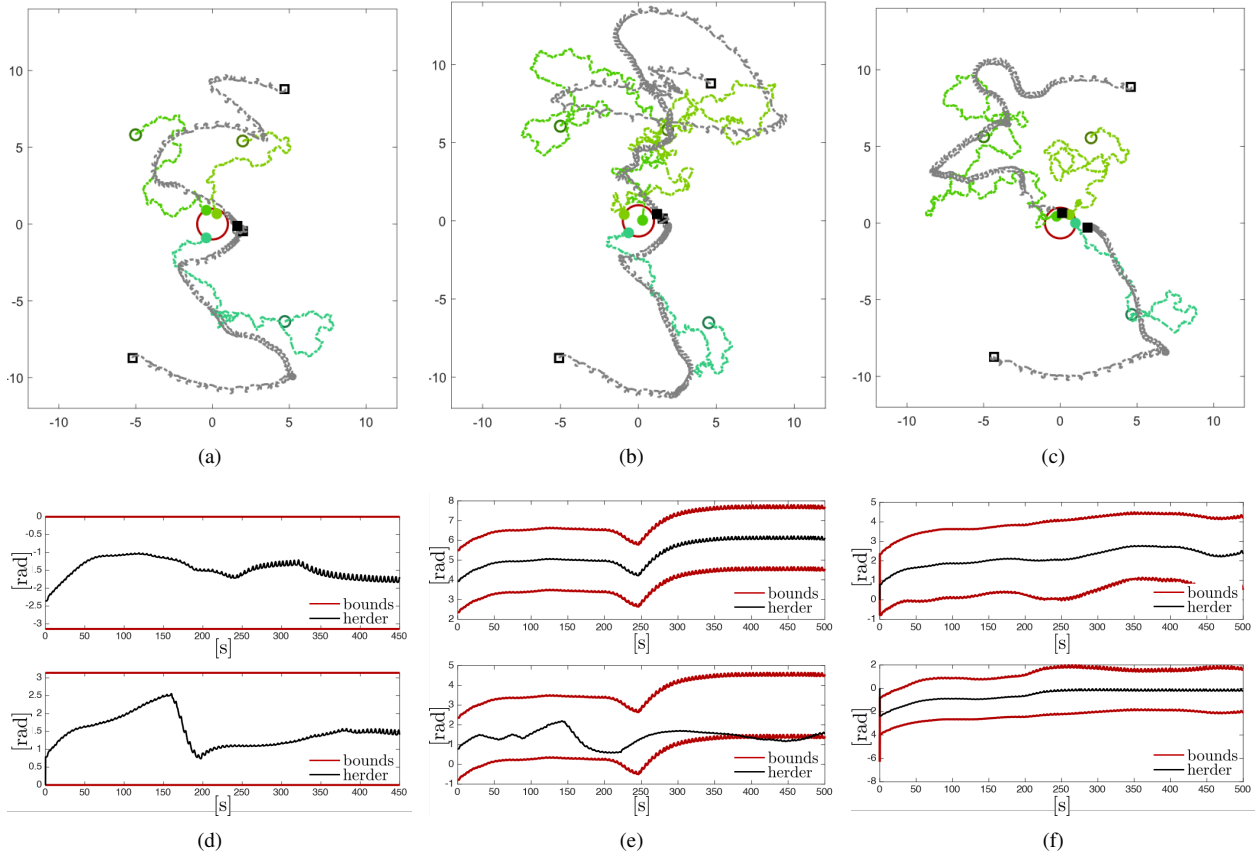


Fig. 6. Top panels show the trajectories of targets (green lines) and herders (black lines) adopting a) static arena partitioning, b) leader-follower and c) peer-to-peer herding strategies simulated in the Gazebo environment. The containment region is depicted as a red circle. Black square marks denote the initial and the final (solid coloured) position of the herders. Green circle marks show the initial and the final (solid coloured) position of the targets. The value of the herding performance metrics computed for each simulation are also reported on top of the corresponding figures. Bottom panels show that all herders are able to collect the targets in less than 500 s by following the angular bounds (red lines) prescribed by the d) static arena partitioning, e) leader-follower and f) peer-to-peer herding strategies.

e) **Behavioural-classification index:** The emerging behaviour of a herder can be evaluated through its power spectra [18]. The behavioural-classification index of the j -th herder is defined as

$$\varphi^{(j)} = \frac{\omega_{\text{freq}}^{(j)} - \omega_c}{|\omega_{\text{freq}}^{(j)} - \omega_c|} \omega_{\text{power}}^{(j)}$$

with $\omega_{\text{freq}}^{(j)}$ being the dominant frequency component, $\omega_{\text{power}}^{(j)}$ the corresponding power, and ω_c the frequency threshold empirically determined at 0.5 Hz, as in [18]. A pair of herders is considered to adopt a search and recovery (SR) behaviour if the behavioural-classification index for both herders $\varphi^{(j)} < 0$, or to adopt a coupled oscillatory containment (COC) behaviour if for both herders $\varphi^{(j)} > 0$.

APPENDIX II MATLAB SIMULATIONS

In all simulations we considered the case of $N_H = 2$ or $N_H = 3$ artificial herders and $N_T = 7$ targets. Moreover, we considered a circular containment region with radius $r^* = 1$ and a buffer region of width $\Delta r^* = 1.0005$. The numerical integration of the differential equations describing

the dynamics of targets and herders has been realised using Euler-Maruyama method [23] in the time interval $[0, T] = [0, 100]$ s with step size $dt = 0.006$ s.

The values of all parameters used in the simulation were chosen as in [18]. Collision detection radius $r_c = 0.0001$, coefficients of diffusion and repulsive motion $(\alpha_b, \alpha_r) = (0.005, 1)$, radial damping and stiffness coefficients $(b_r, \epsilon_r) = (11, 98.7)$, angular damping and stiffness coefficients $(b_\theta, \epsilon_\theta) = (11, 62.6)$.

The initial positions of the targets have been set outside the containment region as $\underline{x}_0^{(i)} = 2r^*e^{j\phi_0^{(i)}}$, $\forall i = 1, \dots, N_T$, with $\phi_0^{(i)}$ drawn with uniform distribution in the interval $(-\pi, \pi)$, while the initial positions of herders have been taken on the circle with radius $4r^*$ and with angular displacement $(2\pi)/N_H$. Furthermore, collision avoidance forces between target agents was also considered in the numerical simulations. To avoid that perfect alignment between the herder and the chased target may cause the target to move away from the goal region, a circumnavigation force $u_{\perp}^{(j)}(t)$ can be added to the dynamics of the herders in (1). This force is orthogonal to the vector $\Delta \underline{x}_{ij} = \underline{x}^{(i)} - \underline{y}^{(j)}$, and its amplitude depends on the angle ψ_{ij} between $\Delta \underline{x}_{ij}$ and $\underline{y}^{(j)}$, such that

it is maximum when the two vectors are parallel ($\psi_{ij} = \pi$) and zero when they are anti-parallel ($\psi_{ij} = 0$). Specifically, it is defined as:

$$u_{\perp}^{(j)}(t) = \bar{U} \cdot v(t) \cdot \cos^2\left(\frac{\psi_{ij}}{2}\right) \frac{\Delta x_{ij}^{\perp}}{\|\Delta x_{ij}\|},$$

where $\bar{U} \in \mathbb{R}_{>0}$ is the maximum amplitude, and $v \in \{-1, 1\}$, whose value depends on which halves of the assigned sector the herder is in, to guarantee that the target is always pushed toward the interior of the sector.

APPENDIX III ROS SIMULATIONS

The mobile robots used for both target and herder agents have been designed as Pioneer 3-DX robots driven by the differential drive controller provided in the set of ROS packages (`gazebo-ros-pkgs`) that allows the integration of Gazebo and ROS.

The environment and the robots share information through an exchange of messages that occurs publishing and subscribing to one or more of the available topics. The target agents collect odometric information from all the herders in the environment. The herder agents subscribe to the ID of the target to-be-chased and collect its position. The robots published message is a velocity control input w.r.t. the robot's reference system to the differential drive of the robot: a translation v along x -axis and a rotation ω around z -axis of the robot. The reference trajectory $\underline{y}^*(t) = [r^* \cos \theta^*, r^* \sin \theta^*]^T$, generated as in Sec. III-IV, is followed by each robot by means of the Cartesian regulator

$$\begin{aligned} v &= -k_1(\underline{y} - \underline{y}^*) [\cos \Phi \quad \sin \Phi] \\ \omega &= k_2(\theta^* - \Phi + \pi) \end{aligned}$$

where $\Phi(t)$ denotes the robot orientation w.r.t. the global reference system. The gains $k_1 = 0.125$ and $k_2 = 0.25$ have been tuned trial-and-error to achieve smooth robot movements. The initial position of the agents have been set as in Appendix II.

The target selection strategies (Sec. IV-B) are processed in an ad-hoc ROS node. It subscribes to the odometry topic; computes the user-chosen strategy (i.e. global, static arena partitioning, leader-follower or peer-to-peer); and publishes a custom message with the ID of the targets to-be-chased on the `/herder/chased.target` topic. The custom message is an array of integer numbers, its j -th element corresponds to the target chased by the j -th herder robot.

The Gazebo-ROS simulations were run on Ubuntu 18.0404 LTS hosted on a VirtualMachine with a 10GB RAM with ROS Melodic distribution and Gazebo 9.13.0.

ACKNOWLEDGEMENTS

The authors wish to acknowledge support from the Macquarie Cotutelle (Industrial and International Leverage Fund) Award and International Macquarie University Research Excellence Scholarship Scheme for supporting Fabrizia Auletta's work. This research was supported, in part, by Australian Research Council Future Fellowship (FT180100447) awarded to Michael Richardson. They also wish to thank Prof. Fabrizio Caccavale from the University of Basilicata, Italy for his advice during the preparation of this article and Dr. Jonathan Cacace from the University of Naples, Italy for his support with ROS.

REFERENCES

- [1] R. R. Murphy, "Human-robot interaction in rescue robotics," *IEEE Trans. on Systems, Man, and Cybernetics, Part C*, vol. 34, no. 2, pp. 138–153, 2004.
- [2] P. Trautman, J. Ma, R. M. Murray, and A. Krause, "Robot navigation in dense human crowds: Statistical models and experimental studies of human robot cooperation," *Int. J. Rob. Res.*, vol. 34, no. 3, pp. 335–356, 2015.
- [3] R. Vaughan, N. Sumpter, J. Henderson *et al.*, "Experiments in automatic flock control," *Rob. Auton. Syst.*, vol. 31, no. 1-2, pp. 109–117, 2000.
- [4] A. A. Paranjape, S. Chung, K. Kim, and D. H. Shim, "Robotic herding of a flock of birds using an unmanned aerial vehicle," *IEEE Trans. Rob.*, vol. 34, no. 4, pp. 901–915, 2018.
- [5] M. A. Haque, A. R. Rahmani, and M. B. Egerstedt, "Biologically inspired confinement of multi-robot systems," *Int. J. of Bio-Inspired Computation*, vol. 3, no. 4, pp. 213–224, 2011.
- [6] J.-M. Lien, O. Bayazit, R. Sowell *et al.*, "Shepherding behaviors," in *Proc. of the IEEE Inter. Conf. on Rob. and Autom.*, 2004, pp. 4159–4164.
- [7] D. Strombom, R. P. Mann, A. M. Wilson *et al.*, "Solving the shepherding problem: heuristics for herding autonomous, interacting agents," *J. R. Soc. Interface*, vol. 11, p. 20140719, 2014.
- [8] P. Kachroo, S. Shediad, J. Bay, and H. Vanlandingham, "Dynamic programming solution for a class of pursuit evasion problems: the herding problem," *IEEE Trans. on Systems, Man and Cybernetics, Part C*, vol. 31, no. 1, pp. 35–41, 2001.
- [9] R. Escobedo, A. Ibañez, and E. Zuazua, "Optimal strategies for driving a mobile agent in a "guidance by repulsion" model," *Commun. Nonlinear Sci. Numer. Simul.*, vol. 39, pp. 58 – 72, 2016.
- [10] P. Deptula, Z. I. Bell, F. M. Zegers *et al.*, "Single Agent Indirect Herding via Approximate Dynamic Programming," in *Proc. of the IEEE Conf. on Decision and Control*, 2018, pp. 7136–7141.
- [11] D. Ko and E. Zuazua, "Asymptotic behavior and control of a "guidance by repulsion" model," *arXiv preprint arXiv:1911.01133*, 2019.
- [12] A. Pierson and M. Schwager, "Controlling Noncooperative Herds with Robotic Herders," *IEEE Trans. on Robotics*, vol. 34, no. 2, pp. 517–525, 2018.
- [13] R. A. Licitra, Z. D. Hutcheson, E. A. Doucette, and W. E. Dixon, "Single Agent Herding of n-Agents: A Switched Systems Approach," *IFAC-PapersOnLine*, vol. 50, no. 1, pp. 14 374–14 379, 2017.
- [14] R. A. Licitra, Z. I. Bell, E. A. Doucette, and W. E. Dixon, "Single Agent Indirect Herding of Multiple Targets: A Switched Adaptive Control Approach," *IEEE Control Syst. Lett.*, vol. 2, no. 1, pp. 127–132, 2018.
- [15] R. A. Licitra, Z. I. Bell, and W. E. Dixon, "Single-agent indirect herding of multiple targets with uncertain dynamics," *IEEE Trans. on Robotics*, vol. 35, no. 4, pp. 847–860, 2019.
- [16] P. Nalepka, C. Riehm, C. B. Mansour *et al.*, "Investigating strategy discovery and coordination in a novel virtual sheep herding game among dyads," in *Proc. of the 37th Annual Meeting of the Cognitive Science Society*, 2015, pp. 1703–1708.
- [17] P. Nalepka, M. Lamb, R. W. Kallen *et al.*, "First step is to group them: Task-dynamic model validation for human multiagent herding in a less constrained task," in *Proc. of the 39th Annual Meeting of the Cognitive Science Society*, 2017, pp. 2784–2789.
- [18] P. Nalepka, R. W. Kallen, A. Chemero *et al.*, "Herd Those Sheep: Emergent Multiagent Coordination and Behavioral-Mode Switching," *Psychological Science*, vol. 28, no. 5, pp. 630–650, 2017.
- [19] P. Nalepka, M. Lamb, R. W. Kallen *et al.*, "Human social motor solutions for human-machine interaction in dynamical task contexts," *PNAS*, vol. 116, no. 4, pp. 1437–1446, 2019.
- [20] M. Bürger, G. Notarstefano, F. Allgöwer, and F. Bullo, "A distributed simplex algorithm and the multi-agent assignment problem," *Proc. of the American Control Conference*, pp. 2639–2644, 2011.
- [21] Stanford Artificial Intelligence Laboratory *et al.*, "Robotic operating system." [Online]. Available: <https://www.ros.org>
- [22] M. Robots, "Pioneer 3 - operations manual." Available at https://www.inf.ufrgs.br/~prestes/Courses/Robotics/manual_pioneer.pdf (2020/08/11).
- [23] D. J. Higham, "An algorithmic introduction to numerical simulation of stochastic differential equations," *SIAM Review*, vol. 43, no. 3, pp. 525–546, 2001.